Synthesis, characterization and ethylene polymerisation of 9,10-phenanthrenequinone-based nickel(II)-α-diimine complexes

Lidong Li*, Manseong Jeon, Sang Youl Kim

Polyolefin Materials Research Center, Department of Chemistry and School of Molecular Science (BK21), Korea Advanced Institute of Science and Technology (KAIST), 373-1, Guseong-dong, Yuseong-Gu, Daejeon 305-701, South Korea

ABSTRACT

Two 9,10-phenanthrenequinone-based α-diimine ligands (N,N′Z, N,N′E)-N,N′-(phenanthrene-9,10-diylidene)bis(2,6-dimethylaniline) (**1**) and (Z)-2,6-dimethyl-N-((E)-10-methylbenzo[f]phenanthro[10,1-bc]azepin-8(14H)-ylidene)aniline (**2**), were prepared by condensation of 2,6-dimethylaniline and 9,10-phenanthrenequinone in the presence of the TiCl$_4$/1,4-diazabicyclo[2.2.2]octane catalytic system in a one-pot reaction. It was experimentally demonstrated that a reaction temperature increase favors the formation of ligand **2**. Nickel dibromide complexes **3** and **4** were synthesized from ligands **1** and **2**, respectively, and both showed high productivities as catalysts for polymerisation of ethylene. Complex **3** yielded ultrahigh molecular weight polyethylenes at low temperature (e.g., 1.26×10^6 g/mol at −15 °C), which are significantly higher than those produced by the corresponding 2,3-butanedione- or acenaphthenequinone-based α-diimine nickel complexes. Complex **4** produced polyethylenes with relatively lower molecular weights, when compared to **3**. It was shown that the catalyst structure and reaction conditions, like the reaction temperature and concentration of activator (MAO), have substantial influence on the polymerisation activities and molecular weights and microstructures of the resulting polymers.

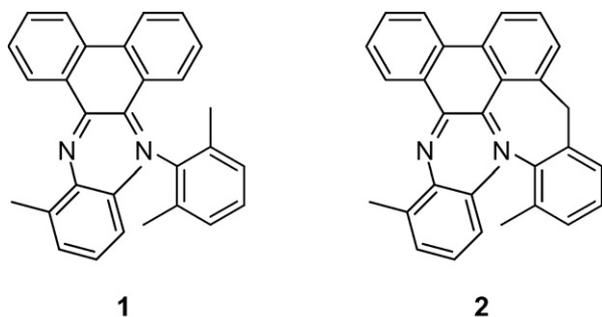© 2009 Elsevier B.V. All rights reserved.

1. Introduction

In the last decade, late transition metal complexes have attracted increased interests in the field of olefin addition polymerisation [1]. Compared to the early Ziegler-Natta catalysts and metallocenes, late transition metal complexes show better tolerance to the functional groups, which make them have an ability to form copolymers with a variety of polar-functionalized comonomers, e.g., methyl acrylate (MA) [2a], methyl methacrylate (MMA) [2b] and ω-unsaturated fatty acid methyl esters [2c]. In addition, due to their less oxophilicities, these complexes can run the polymerisation in polar media, and even in emulsion or water [3]. Marked chain isomerisation mechanism ("chain walking") of nickel and palladium complexes allows them to produce polymers with a broad spectrum of branching topologies, ranging from relatively linear to hyperbranched or dendritic [4].

The design of ligands is very important to determine the performance of late transition metal complexes, and much research has been dedicated to this subject [1a,1b]. It has been suggested that, in the case of Ni^{II}- and Pd^{II}-α-diimine complexes, the increase of the steric demands of the aryl ring substituents can dramatically retard bimolecular deactivation and lead to increased activities of catalysts and molecular weights of the resulting polymers. Guan and coworkers [5] reported cyclophane-based nickel and palladium complexes, in which the rigid frameworks of the ligands completely block the axial faces of the metals and prohibit free rotation of the aryl-nitrogen bonds so that these complexes can polymerise olefin at elevated temperature with high activities. Ionkin and Marshall [6] introduced sterically large 5-methylfuran and benzofuran substituents on the aryl rings of α-diimine ligands, which lead to highly active nickel complexes producing polyethylenes with ultrahigh molecular weights. Müller et al. [7] demonstrated that the introduction of dendritic substituents on the bidentate P,O ligands of SHOP nickel complexes can efficiently hamper bimolecular deactivation, and substantially improve the activities of the final complexes. More recently, Grubbs and coworkers [8] reported the salicylaldimine-based neutral nickel complexes. It has been shown that the sterically demanding substituents have similar influences on the neutral nickel complexes to those on the α-diimine nickel complexes.

* Corresponding author at: Centro de Química Estrutural, Departamento de Engenharia Química e Biológica, Instituto Superior Técnico, Av. Rovisco Pais, 1049-001 Lisboa, Portugal. Tel.: +351 21 841 7713; fax: +351 21 841 9612.
E-mail address: dick_lld@hotmail.com (L. Li).

1 **2**

In the present work, we reported two new 9,10-phenanthrenequinone-based α-diimine ligands (**1** and **2**), and tested the catalytic performance of two nickel complexes (**3** and **4**), which were formed from ligands **1** and **2**, respectively, on ethylene polymerisation.

2. Experimental

2.1. General considerations

All manipulations of air and/or water sensitive compounds were conducted under argon atmosphere using the standard Schlenk techniques. Infrared (IR) spectra were recorded on a Bruker Equinox55 FT-IR spectrometer. Mass spectra (MS) were recorded on a VG Autospec Ultima MS spectrometer. ^{1}H NMR spectra were recorded on a Bruker Avance-400 NMR spectrometer. Chemical shifts are reported relative to the residual solvent (CDCl$_3$, $\delta(^1H) = 7.24$, $\delta(^{13}C) = 77.0$; tetrachloroethane-d$_2$, $\delta(^1H) = 6.0$). The branching of polymer was measured by ^{1}H NMR spectroscopy in tetrachloroethane-d$_2$ at 120 °C. The degrees of branching of polymers were calculated from the integrals of the methyl, methylene and methine groups as the following equations:

Branches/1000 C

$$= \frac{S_A(methyl)/3}{S_A(methyl)/3 + S_A(methylene)/2 + S_A(methine)} \times 1000$$

where $S_A(methyl)$, $S_A(methylene)$ and $S_A(methine)$ are the integrals of the methyl, methylene and methine groups of polymers, respectively. Weight-average (Mw) and number-average (Mn) molecular weight and molecular weight distribution (MWD) were measured by gel permeation chromatography (GPC) on a SSC-7100 apparatus, at 145 °C, using the o-dichlorobenzene as the eluent. The calibration curve was determined with polystyrene standards. Glass transition temperature (T_g) and melting temperature (T_m) of polymer samples were determined using a TA-Q100 differential scanning calorimeter at a scanning rate of 10 °C/min.

2.2. Materials

All the solvents were purified prior to use. Toluene (J.T. Baker, USA) and ethyl ether (Junsei Chemical Co., Ltd., Japan) were purified over sodium/benzophenone ketyl, and distilled prior to use. Chlorobenzene (Junsei Chemical Co., Ltd., Japan) and dichloromethane (Junsei Chemical Co., Ltd., Japan) was purified over calcium hydride powder, and distilled prior to use. Polymerisation grade ethylene gases were purified by passing 4 Å molecular sieves column and Ridox® oxygen scavenger (R31-500) column, respectively. 1,4-Diazabicyclo[2.2.2]octane (Dabco) (95%) was purchased from Aldrich and purified by sublimation. MAO (10 wt% in toluene), 9,10-phenanthrenequinone (95%), titanium tetrachloride (99.9%), 2,6-dimethylaniline (99%), and (DME)NiBr$_2$ (DME,

dimethyl ethylene glycol ether) were purchased from Aldrich and used as received.

2.3. Syntheses of ligands and complexes

2.3.1. Synthesis of ligand **1**

To a solution of 2,6-dimethylaniline (14.4 mmol, 1.77 ml) and Dabco (43.2 mmol, 4.85 g) in toluene (30 ml) was added dropwise 14.4 ml of the 1.0 M solution of TiCl$_4$ in toluene over 30 min at 90 °C, followed by addition of a suspension of 9,10-phenanthrenequinone (4.80 mmol, 1.0 g) in 10 ml of toluene. The reaction mixture was heated to reflux (ca. 140 °C) for 24 h. The precipitate was removed by hot filtration. The filtrate was evaporated *in vacuo*. Finally, 1.0 g of deep red crystalline solid was isolated by silica gel column chromatography (hexane/ethyl acetate, 8:1) and recrystallisation in hexane. Yield: 50%. ^{1}H NMR (400 MHz, CDCl$_3$, ppm): 8.34 (d, 1H), 7.92 (m, 2H), 7.60 (t, 1H), 7.51 (t, 1H), 7.39 (t, 1H), 6.99 (br, 2H), 6.92 (t, 1H), 6.87 (t, 1H), 6.83 (br, 3H), 6.73 (d, 1H), 2.06 (s, 6H), 1.39 (s, 6H). ^{13}C NMR (100 MHz, CDCl$_3$, ppm): 159.9, 158.2, 148.8, 147.4, 134.5, 134.0, 133.3, 131.8, 131.3, 129.0, 128.9, 127.8, 127.6, 127.5, 127.3, 126.9, 125.2, 124.8, 124.5, 123.4, 123.0, 122.5, 18.3, 17.1. IR (KBr, cm^{-1}): 1646 (C=N), 1622 (C=N). EI-MS (*m/z*): calcd for C$_{30}$H$_{26}$N$_2$, 414.54; found, 414 [M]$^+$ (14%), 399 [M−CH$_3$]$^+$ (100%).

2.3.2. Synthesis of ligand **2**

The synthetic procedure was similar to that described for ligand **1**, but chlorobenzene was used in place of toluene as solvent and the reflux temperature was raised over 160 °C. An orange crystalline solid was isolated. Yield: 35%. ^{1}H NMR (400 MHz, CDCl$_3$, ppm): 8.42 (d, 1H), 7.92 (d, 1H), 7.81 (d, 1H), 7.55 (m, 3H), 7.21 (d, 1H), 7.04 (t, 1H), 6.97 (br, 3H), 6.86 (d, 1H), 6.77 (t, 1H), 3.58 (d, 1H), 3.20 (d, 1H), 2.40 (s, 3H), 2.19 (s, 3H), 1.84 (s, 3H). ^{13}C NMR (100 MHz, CDCl$_3$, ppm): 161.3, 157.0, 149.2, 143.2, 142.0, 135.2, 134.3, 133.8, 133.6, 132.5, 131.4, 130.9, 129.2, 128.9, 128.7, 128.0, 127.3, 127.0, 126.9, 126.4, 126.1, 124.8, 123.5, 122.4, 122.3, 121.0, 38.7, 18.8, 18.7, 18.4. IR (KBr, cm^{-1}): 1645 (C=N). EI-MS (*m/z*): calcd for C$_{30}$H$_{24}$N$_2$, 412.52; found, 412 [M]$^+$ (62%), 397 [M−CH$_3$]$^+$ (100%).

2.3.3. Synthesis of complex **3**

Ligand **1** (0.50 g, 1.21 mmol) and (DME)NiBr$_2$ (0.37 g, 1.21 mmol) were combined as solids in a flame-dried Schlenk flask. Dichloromethane (50 ml) was added to the solid mixture and the reaction was stirred at room temperature (ca. 20 °C) for 24 h. The solvent was removed *in vacuo* and the residual solid was washed with Et$_2$O several times. Finally, complex **3** was isolated as a brown powder (0.66 g, 86%). Anal. calcd for C$_{30}$H$_{26}$Br$_2$N$_2$Ni: C, 56.92; H, 4.14; N, 4.43. Found: C, 56.55; H, 4.13; N, 4.35.

2.3.4. Synthesis of complex **4**

The synthetic procedure was similar to that described for complex **3**. A brown powder was obtained. Yield: 96%. Anal. calcd for C$_{30}$H$_{24}$Br$_2$N$_2$Ni: C, 57.10; H, 3.83; N, 4.44. Found: C, 57.53; H, 3.52; N, 4.21.

2.4. X-ray crystallography

Single crystals of ligand **2** suitable for X-ray diffraction characterization were grown from a dilute hexane solution at 0 °C. Crystal data was collected in a Bruker AXS-KAPPA APEX II diffractometer equipped with an Oxford Cryosystems open-flow nitrogen cryostat, at 150 K, using graphite monochromated Mo Kα radiation (λ = 0.71069 Å). Cell parameters were retrieved using Bruker SMART software and refined using Bruker SAINT on all observed reflections. Absorption corrections were applied using SADABS [9]. Structure solution and refinement were performed using direct methods with

Table 1
Crystal data and structure refinement for ligand **2**.

Empirical formula	$C_{30}H_{24}N_2$
Formula weight	412.51
Temperature (K)	150(2)
Wavelength (Å)	0.71073
Crystal system, space group	Triclinic, *P*-1
Unit cell dimensions	$a = 8.252$ Å, $\alpha = 76.32°$
	$b = 11.119$ Å, $\beta = 89.20°$
	$c = 12.233$ Å, $\gamma = 86.08°$
Volume (Å³)	1084.0
Z, calculated density (Mg m⁻³)	2, 1.259
Absorption coefficient (mm⁻¹)	0.073
F(0 0 0)	436
Theta range for data collection (°)	2.23–30.97
Index ranges	$-11 \leq h \leq 11$, $-16 \leq k \leq 15$, $-17 \leq l \leq 17$
Reflections collected/unique	38697/6867 [$R_{int} = 0.0471$]
Completeness to theta = 30.97	99.3%
Absorption correction	Semi-empirical from equivalents
Refinement method	Full-matrix least-squares on F^2
Max. and min. transmission	0.9869 and 0.9783
Refinement method	Full-matrix least-squares on F^2
Data/restraints/parameters	6867/0/289
Goodness-of-fit on F^2	0.993
Final *R* indices [$I > 2\sigma(I)$]	$R_1 = 0.0626$, $wR_2 = 0.1902$
R indices (all data)	$R_1 = 0.0857$, $wR_2 = 0.2034$
Largest diff. peak and hole (e. Å⁻³)	0.645 and −0.578

the programs SIR92 [10] and SHELXL [11] both included in the package of programs WINGX-Version 1.70.01 [12]. Non-hydrogen atoms were refined with anisotropic thermal parameters. All hydrogen atoms were inserted in idealized positions and allowed to refine riding in the parent C atoms. All remaining crystal data and refinement parameters are presented in Table 1. The figures were generated using ORTEP-III [13].

CCDC 673942 contains the supplementary crystallographic data for this paper. These data can be obtained free of charge via www.ccdc.cam.ac.uk/data_request/cif, or by emailing data_request@ccdc.cam.ac.uk, or by contacting The Cambridge Crystallographic Data Centre, 12, Union Road, Cambridge CB2 1EZ, UK; fax: +44 1223 336033.

2.5. Ethylene polymerisation

Ethylene polymerisation was conducted in a 50-ml Schlenk flask equipped with vacuum line, ethylene inlet and magnetic stirrer.

The flask was flamed *in vacuo* and back-filled with ethylene. The appropriate amount of toluene and the MAO were injected into the reactor, and the ethylene inlet was opened to make the system saturated by ethylene at a certain reaction temperature. The polymerisation was initiated by addition of the catalyst solution in dichloromethane. After 60 min, the polymerisation was terminated by addition of the acidified methanol. The resulting polyethylene was filtered, washed with a large amount of methanol and dried *in vacuo* at 60 °C.

3. Results and discussion

3.1. Preparation of ligands and complexes

Ligand **1** was prepared by dehydrating condensation of 2,6-dimethylaniline and 9,10-phenanthrenequinone, using the TiCl₄/Dabco system in toluene (Scheme 1). Based on NMR results and comparison with the analogue (*Z,Z*)-9,10-bis(phenylimino)-9,10-dihydrophenanthrene already published [14], it can be concluded that ligand **1** adopts a (*Z,E*) configuration. The two strikingly different methyl peaks (2.05 and 1.39 ppm), obtained by ¹H NMR spectra, correspond to methyl groups on aromatic rings with different configurations, respectively. At the same time, two pairs of different –C=N–C peaks (159.9 and 158.2 ppm) and –C=N–C peaks (148.8 and 147.4), obtained by ¹³C NMR spectra, further indicate that the aromatic rings should be assigned to different configurations with respect to C=N bonds. In the case of ligand **1**, the energetically favored π-stacking in (*Z,Z*) configuration might be retarded by introduction of methyl groups on the ortho positions of the aromatic rings.

Ligand **2** was simultaneously produced along with ligand **1** in a one-pot reaction. Reaction temperature has a significant impact on the selectivity for ligands **1** and **2**. As reaction temperature was controlled at 140–150 °C, using toluene as solvent, the major product was ligand **1** (50%) and a small amount of ligand **2** was isolated as a byproduct (ca. 5%). As the toluene was replaced by chlorobenzene and the reaction temperature was increased to 160–170 °C, ligand **2** became the major product (35%) and the amount of ligand **1** formed decreased to ~10%. This indicates that ligand **1** is preferentially formed at a relatively lower reaction temperature, and that a reaction temperature increase favors the formation of ligand **2**. Crystals of ligand **2**, suitable for single crystal X-ray diffraction, were grown from a dilute solution in hexane at 0 °C (Fig. 1). As shown in Fig. 1, the two aromatic rings of ligand **2** adopt (*Z,E*) configurations
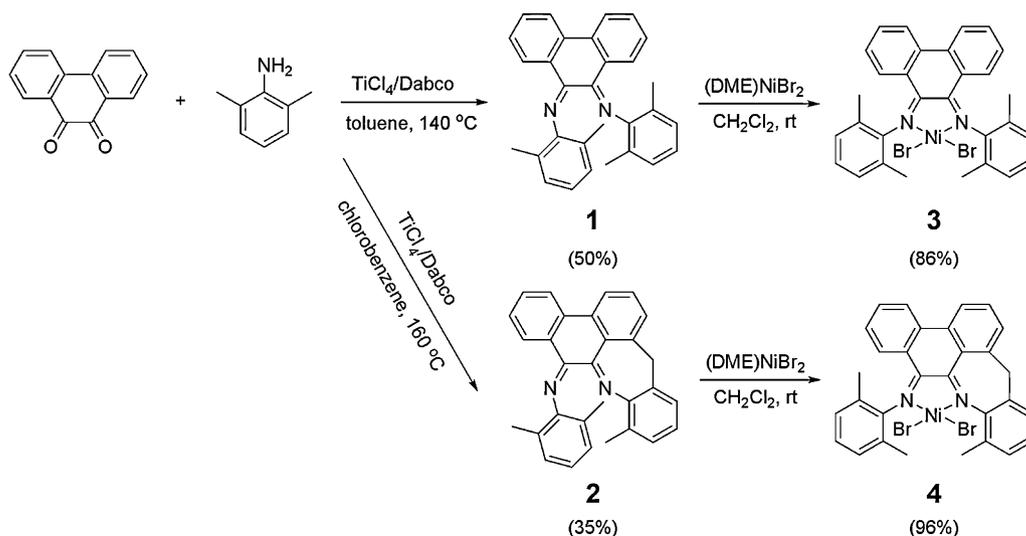
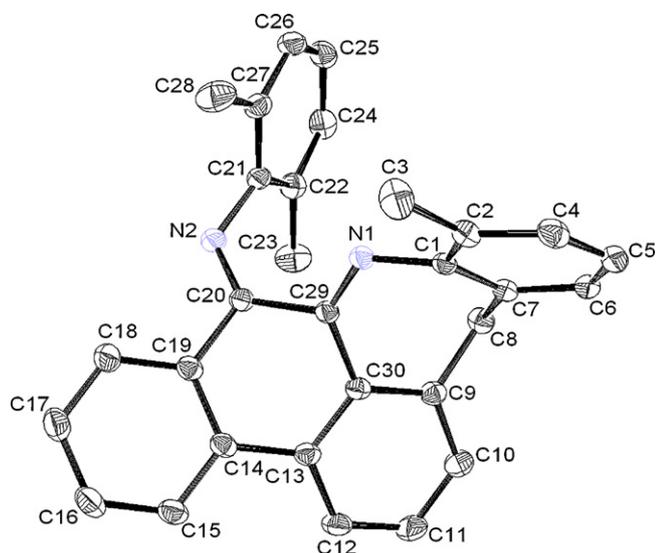**Scheme 1.** Syntheses of the ligands and the complexes.

Fig. 1. ORTEP view of crystal structure of ligand **2** with 50% probability displacement ellipsoids. H-atoms are omitted for clarity.

with respect to the C=N bonds, which is in agreement with the NMR result. The mechanism for the formation of ligand **2** is still unclear, and the subject is being investigated in our laboratory.

Reaction of ligands **1** and **2** with (DME)NiBr$_2$ in dichloromethane, at room temperature, resulted in the formation of the nickel complexes **3** and **4**, in considerably good yields (86% and 96%, respectively).

3.2. Ethylene polymerisation

3.2.1. Effects of the catalysts

Complexes **3** and **4** are both catalytically active towards ethylene polymerisation, in the presence of MAO as activator. The polymerisation data are summarized in Tables 2 and 3. These two nickel complexes exhibit high activities for ethylene polymerisation, which are comparable to the typical α-dimine nickel complexes [1c]. For example, the catalytic activity of complex **3** can reach

the value of 2.28×10^6 g of PE mol^{-1} of Ni h^{-1} (entry 7 in Table 2). Polyethylenes formed using complex **3** as a catalyst contain similar extent of branching to those obtained using the typical α-dimine nickel complexes, e.g., 29–35 branches/1000 C (entries 16–19 in Table 2) versus 29 branches/1000 C ([ArN=C(H)–C(H)=NAr]NiBr$_2$, Ar = 2,6-dimethylphenyl, 1 atm ethylene pressure, 25 °C [1c]). Complex **4** produces polyethylenes with higher extent of branching compared to complex **3** (Table 3).

As shown in Tables 2 and 3, under the same polymerisation conditions, complex **3** displays higher polymerisation activities than complex **4**, and polyethylenes formed using complex **3** contain molecular weights approximately 5 times larger than those obtained using complex **4**. In addition, as the polymerisation temperature increases, the activities of complex **3** decrease slower than those of complex **4**, indicating that the former is more thermally stable than the latter. All of these results may be attributed to the fact that complex **3** has more steric protection on the axial faces of the coordination plane than complex **4**. Compared to **3**, the methylene linkage of complex **4** makes the N-aryl group deviate the perpendicular orientation to the coordination plane, and renders the substituents of the N-aryl group away from the axial faces, which lead to a substantial decrease of the steric protection on the axial faces of the coordination plane. On the basis of the proposed mechanism [1], the steric bulk on the axial faces of the coordination plane may inhibit bimolecular deactivation of catalysts and suppress associative chain transfer or chain transfer to ethylene monomer. Therefore, complex **3** is more active for ethylene polymerisation and more stable against reaction temperature than complex **4**, and the resulting polymers formed by complex **3** have higher molecular weights than those obtained by complex **4**.

It is worth to note that complex **3** produces polyethylenes with ultrahigh molecular weights at lower polymerisation temperature, e.g., $1.26–2.14 \times 10^6$ g/mol at −15 °C (entries 4–7 in Table 2), and 1.27 and 1.01×10^6 g/mol at 0 °C (entries 11 and 14 in Table 2). Additionally, molecular weights of polyethylenes formed by complex **3** are much higher than those obtained by the structurally similar Brookhart's α-diimine nickel complexes, e.g., $(2.6–12.7) \times 10^5$ g/mol at 0 °C (entries 8–14 in Table 2) versus 4.3 and 17×10^4 g/mol at 0 °C for [ArN=C(R)–C(R)=NAr]NiBr$_2$ (Ar = 2,6-dimethylphenyl, R = H or Me) (entries 13 and 15 in Table 1

Table 2
Ethylene polymerisation catalyzed by the **3**/MAO system[a].

Entry	Catalyst (µmol)	MAO (mmol/equiv.)	Temp. (°C)	Yield (g)	Activity (10^5 g/mol Ni h)	Mn[b] (10^5 g/mol)	Mw/Mn[b]	Branches/1000 C[c]	Thermal anal.[d] (°C)
1	4.0	0.2/50	−15	0.46	1.15	5.0	3.7	3.0	132.9 (T_m)
2	4.0	0.4/100	−15	0.86	2.15	4.9	3.6	3.0	131.7 (T_m)
3	2.0	0.5/250	−15	1.11	5.55	1.1	8.5	2.0	132.5 (T_m)
4	1.0	0.5/500	−15	1.27	12.70	16.9	2.0	3.0	130.0 (T_m)
5	1.0	1.0/1000	−15	1.05	10.50	12.6	2.1	−[e]	132.4 (T_m)
6	0.5	1.0/2000	−15	0.64	12.80	14.2	2.0	−[e]	131.7 (T_m)
7	0.5	1.5/3000	−15	1.14	22.80	21.4	1.8	2.0	130.6 (T_m)
8	2.0	0.1/50	0	0.97	4.85	2.6	6.4	7.0	124.6 (T_m)
9	2.0	0.2/100	0	1.58	7.90	6.4	3.6	10.0	123.4 (T_m)
10	2.0	0.5/250	0	1.71	8.55	9.1	2.6	7.0	122.9 (T_m)
11	1.0	0.5/500	0	1.28	12.80	12.7	2.4	4.0	125.9 (T_m)
12	1.0	1.0/1000	0	1.19	11.90	5.9	3.9	7.0	124.5 (T_m)
13	1.0	2.0/2000	0	1.58	15.80	3.3	5.9	4.0	124.9 (T_m)
14	1.0	3.0/3000	0	1.52	15.20	10.1	2.2	8.0	121.7 (T_m)
15	2.0	0.5/250	30	0.20	1.00	3.2	2.4	21.0	103.6 (T_m)
16	2.0	1.0/500	30	0.84	4.20	2.2	2.7	35.0	91.4 (T_m)
17	2.0	2.0/1000	30	1.28	6.40	2.2	2.8	35.0	82.6 (T_m)
18	1.0	2.0/2000	30	1.26	12.60	2.6	2.5	30.0	94.9 (T_m)
19	1.0	3.0/3000	30	1.47	14.70	3.4	2.5	29.0	93.7 (T_m)

[a] General polymerisation conditions: toluene as solvent, total volume (40 ml), ethylene pressure (1.20 atm), reaction time (1.0 h).

[b] Determined by GPC.

[c] Determined by ^{1}H NMR.

[d] Determined by DSC.

[e] Not detectable.

Table 3
Ethylene polymerisation catalyzed by the **4**/MAO system[a].

Entry	Catalyst (μmol)	MAO (mmol/equiv)	Temp. (°C)	Yield (g)	Activity (10^5 g/mol Ni h)	Mn[b] (10^5 g/mol)	Mw/Mn[b]	Branches/1000C[c]	Thermal anal.[d] (°C)
1	4.0	0.2/50	−15	0.64	1.60	1.2	2.4	5.0	128.2 (T_m)
2	4.0	0.4/100	−15	0.92	2.30	1.4	2.8	4.0	127.3 (T_m)
3	2.0	0.5/250	−15	0.59	2.95	1.8	2.3	4.0	129.0 (T_m)
4	2.0	1.0/500	−15	0.76	3.80	1.0	3.1	4.0	128.7 (T_m)
5	2.0	2.0/1000	−15	0.87	4.35	1.7	2.4	5.0	128.7 (T_m)
6	1.0	2.0/2000	−15	0.49	4.90	1.2	3.0	4.0	128.6 (T_m)
7	0.5	1.5/3000	−15	0.25	5.00	2.4	2.2	4.0	129.7 (T_m)
8	4.0	0.2/50	0	0.99	2.48	0.9	3.9	15.0	119.3 (T_m)
9	4.0	0.4/100	0	1.44	3.60	1.3	3.2	15.0	119.0 (T_m)
10	2.0	0.5/250	0	0.84	4.20	1.4	3.9	13.0	120.6 (T_m)
11	2.0	1.0/500	0	0.97	4.85	1.5	2.9	11.0	121.0 (T_m)
12	2.0	2.0/1000	0	1.06	5.30	1.3	3.9	12.0	119.7 (T_m)
13	1.0	2.0/2000	0	0.66	6.60	2.0	3.0	11.0	120.0 (T_m)
14	1.0	3.0/3000	0	0.69	6.90	2.0	3.1	13.0	119.3 (T_m)
15	2.0	2.0/1000	30	0.31	1.55	0.4	2.0	69.0	−44.1 (T_g), 41.4 (T_m)
16	2.0	4.0/2000	30	0.35	1.75	0.4	2.1	67.0	−49.0 (T_g), 44.3 (T_m)
17	2.0	6.0/3000	30	0.36	1.80	0.4	2.0	69.0	−47.6 (T_g), 45.4 (T_m)

[a] General polymerisation conditions: toluene as solvent, total volume (40 ml), ethylene pressure (1.20 atm), reaction time (1.0 h).
[b] Determined by GPC.
[c] Determined by ^{1}H NMR.
[d] Determined by DSC.

[1c]), and $(2.2–3.4) \times 10^5$ g/mol at 30 °C (entries 15–19 in Table 2) versus 1.43×10^4 g/mol at 35 °C for [ArN=C(An)–C(An)=NAr]NiBr$_2$ (Ar = 2,6-dimethylphenyl) (entry 6 in Table 1 [1f]). This suggests that the α-diimine nickel complexes based on 9,10-phenanthrenequinone (**3**) can introduce more steric demands on the axial faces than those based on 2,3-butanedione and acenaphthenequinone.

Another striking feature that can be observed from Tables 2 and 3 is that the extents of branching of polyethylenes obtained by complex **4** are approximately two times higher than those obtained by complex **3**, which exhibits a substantially different trend from the Brookhart's α-dimine nickel complexes [1c,1f]. In the case of the latter, the extent of branching increases with the bulk of the aryl subsituents, that is to say, an increase of the steric demands on the axial faces of the coordination plane will yield a polymer with higher branching. Brookhart and his coworkers [1f] suggested that, since the propagation rate is suppressed by bulky substituents more than the rate of chain running, more chain running and branching can occur in the catalysts that bear bulky substituents, in comparison with those that possess less bulky substituents. However, in the case of complexes **3** and **4**, polyethylenes formed by complex **4**, with less steric demands on the axial faces, have more branching than those obtained by complex **3**, with more steric demands. This is possibly due to the asymmetric geometry of complex **4**, which not only enhances the propagation rate but also favors the chain running.

3.2.2. Effects of the polymerisation conditions

The effects of the Al/Ni molar ratio and the reaction temperature on polymerisation activities are summarized in Fig. 2. As displayed in Fig. 2, the catalytic activities of complex **3** are much higher than those of complex **4**. Since increasing the concentration of MAO may improve the number of the active species in the reaction and contribute to the stabilization of the formed active species [15], the polymerisation activities progressively increase with the Al/Ni molar ratio (Fig. 2). In addition, it is worth to note that, due to enhanced tolerance of nickel complexes to moisture and polar functionalities, complexes **3** and **4** can be activated by a quite small amount of MAO to promote ethylene polymerisation, e.g., Al/Ni = 50 (entries 1 and 8 in Tables 2 and 3). This gains a marked advantage over the early transition metal catalysts (e.g., metallocene) since it avoids the use of a large amount of MAO which is commercially expensive. Fig. 2 shows that the Al/Ni molar ratio of 500 is an optimum value, which allows to maintain the high activities and simultaneously to reduce the amount of MAO used. In fact, the activities dramatically reduce as the Al/Ni molar ratio goes below 500, whereas they slightly increase as the ratio is above 500. Several factors may play roles over determining the effect of temperature on the polymerisation activity, which involve stabilities of complexes and the formed active species in the reaction, solubility of the monomer in media, and the influence of the reaction temperature on the propagation rate. In the case of complexes **3** and **4**, these factors render the complexes more active at 0 °C than at −15 °C or 30 °C, and the activities at 0 °C and −15 °C are noticeably higher than those at 30 °C (Fig. 2).

Both the Al/Ni molar ratio and the reaction temperature have influences on the molecular weights of the resulting polymers, as shown in Fig. 3. The molecular weights decrease as the polymerisation temperature increases, for both **3** and **4**, since the higher temperature more favors the chain transfer than the chain propagation. The Al/Ni molar ratio hardly influence the molecular weights of polymers obtained by complex **4**, at various temperatures, and complex **3** at 30 °C. However, at −15 °C and 0 °C, the molecular
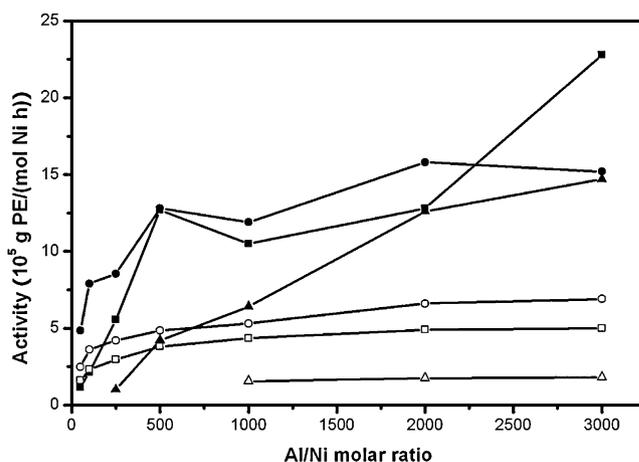

Fig. 2. Effects of the Al/Ni molar ratio and the reaction temperature on the polymerisation activities promoted by complexes **3** and **4**. Solid, **3**; open, **4**; square, −15 °C; circle, 0 °C; up triangle, 30 °C.
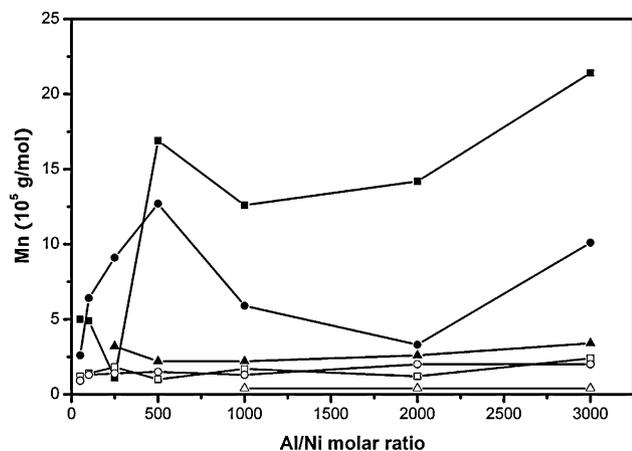
Fig. 3. Effects of the Al/Ni molar ratio and the reaction temperature on the molecular weights of polyethylenes prepared by complexes **3** and **4**. Solid, **3**; open, **4**; square, −15 °C; circle, 0 °C; up triangle, 30 °C.

weights of polymers obtained by complex **3** pronouncedly vary with the Al/Ni molar ratio. The reason for this effect is still unclear. It might be related to the fact that, for the more catalytically active complex **3**, the lower reaction temperatures result in the precipitation of the formed polymers with relatively higher molecular weights from the reaction solution, which heterogenizes the reaction system (although a lower concentration of complex was used, as the Al/Ni molar ratio was increased, in order to avoid this effect).

The effects of the Al/Ni molar ratio and the temperature on the extents of branching of the resulting polymers are shown in Fig. 4. It can be seen that the branching markedly increases as the reaction temperature increases. This trend can also be clearly observed by analysis of the ^{1}H NMR spectra in Fig. 5. The small doublet observed at $\delta = 0.95$ ppm, which is assigned to the methyl branches, becomes more intense with the temperature increase, when compared with the methylene resonances at $\delta = 1.37$ ppm. At the same time, the methine resonances, which are observed as broad resonances at $\delta = 1.22$ ppm, increase with the reaction temperature. Furthermore, the fact that the methyl resonances are split into doublets indicates that these polyethylenes mainly have CH_3 branches. The Al/Ni molar ratio has an insignificant influence on the branching degree, just like it was found for the Brookhart α-dimine nickel complexes [1c,1f].
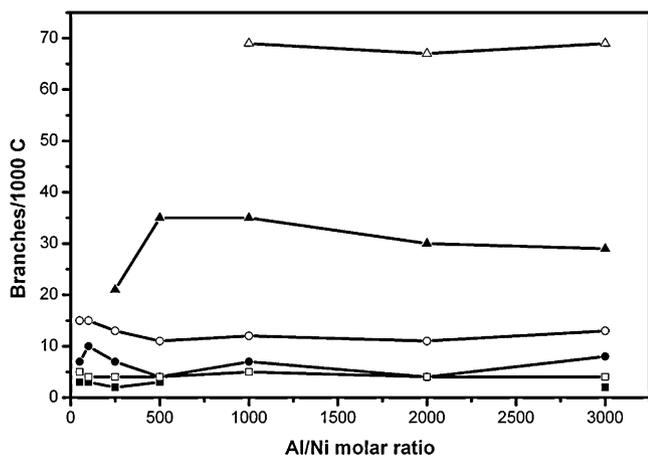

Fig. 4. Effects of the Al/Ni molar ratio and the reaction temperature on the degree of branching of polyethylenes prepared by complexes **3** and **4**. Solid, **3**; open, **4**; square, −15 °C; circle, 0 °C; up triangle, 30 °C.
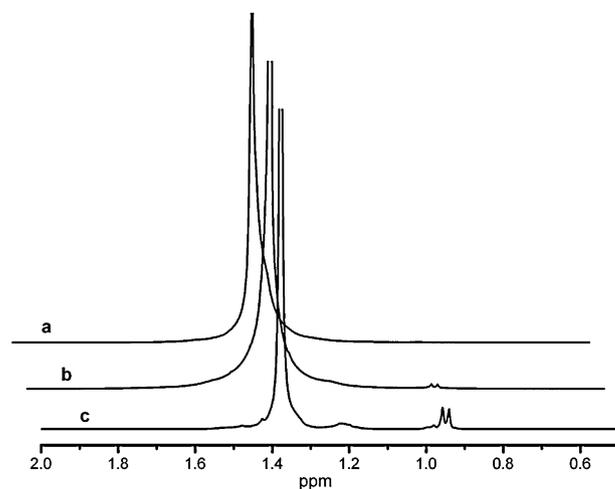

Fig. 5. ^{1}H NMR spectra of polyethylenes prepared by complex **3** at different temperatures. a, b and c correspond to entries 5, 12 and 17 in Table 2, respectively.

4. Conclusions

Two novel 9,10-phenanthrenequinone-based α-diimine ligands **1** and **2**, prepared by condensation of 9,10-phenanthrenequinone with 2,6-dimethylaniline in the presence of the TiCl₄/Dabco system in a one-pot reaction, are reported. A higher reaction temperature favors the formation of ligand **2**. Nickel complexes **3** and **4** are prepared from ligands **1** and **2**, respectively, and both show good activities for ethylene polymerisation, in the presence of MAO. The final polyethylenes obtained by complexes **3** and **4** have comparable structures of branching to the Brookhart's α-diimine nickel complexes. Complex **3** exhibits a higher polymerisation activity than complex **4**, and yields polyethylenes with higher molecular weights and less extents of branching. Additionally, complex **3** produces polyethylenes with ultrahigh molecular weights, at a relatively lower polymerisation temperature, e.g., $(1.26–2.14) \times 10^6$ g/mol at −15 °C (entries 4–7 in Table 1). It was demonstrated that the reaction conditions, e.g., the reaction temperature and the concentration of activator (MAO), have significant influences on the polymerisation activities and the degrees of branching of the resulting polymers.

Acknowledgments

Appendix A. Supplementary data

Supplementary data associated with this article can be found, in the online version, at doi:10.1016/j.molcata.2009.01.007.

References

[1] (a) S.D. Ittel, L.K. Johnson, Chem. Rev. 100 (2000) 1169–1203;
(b) V.C. Gibson, S.K. Spitzmesser, Chem. Rev. 103 (2003) 283–315;
(c) L.K. Johnson, C.M. Killian, M. Brookhart, J. Am. Chem. Soc. 117 (1995) 6414–6415;
(d) C.M. Killian, D.J. Tempel, L.K. Johnson, M. Brookhart, J. Am. Chem. Soc. 118 (1996) 11664–11665;
(e) D.J. Tempel, L.K. Johnson, R.L. Huff, P.S. White, M. Brookhart, J. Am. Chem. Soc. 122 (2000) 6686–6700;
(f) D.P. Gates, S.A. Svejda, E. Onate, C.M. Killian, L.K. Johnson, P.S. White, M. Brookhart, Macromolecules 33 (2000) 2320–2334;
(g) B.L. Small, M. Brookhart, A.M. Bennett, J. Am. Chem. Soc. 120 (1998) 4049–4050;

(h) G.J.P. Britovsek, V.C. Gibson, B.S. Kimberley, P.J. Maddox, S.J. McTavish, G.A. Solan, A.J.P. White, D.J. Williams, Chem. Commun. (1998) 849–850.

[2] (a) L.K. Johnson, S. Mecking, M. Brookhart, J. Am. Chem. Soc. 118 (1996) 267–268;
(b) X.-F. Li, Y.-G. Li, Y.-S. Li, Y.-X. Chen, N.-H. Hu, Organometallics 24 (2005) 2502–2510;
(c) S. Warwel, B. Wiege, E. Fehling, M. Kunz, Macromol. Chem. Phys. 202 (2001) 849–855.

[3] (a) F.M. Bauers, S. Mecking, Angew. Chem. Int. Ed. 40 (2001) 3020–3022;
(b) S. Mecking, A. Held, F.M. Bauers, Angew. Chem. Int. Ed. 41 (2002) 544–561;
(c) A. Held, F.M. Bauers, S. Mecking, Chem. Commun. (2000) 301–302;
(d) A. Held, S. Mecking, Chem. Eur. J. 6 (2000) 4623–4629;
(e) I. Göttker-Schnetmann, B. Korthals, S. Mecking, J. Am. Chem. Soc. 128 (2006) 7708–7709;
(f) F.M. Bauers, S. Mecking, Macromolecules 34 (2001) 1165–1171;
(g) R. Soula, C. Novat, A. Tomov, R. Spitz, J. Claverie, X. Drujon, J. Malinge, T. Saudemont, Macromolecules 34 (2001) 2022–2026;
(h) R. Soula, B. Saillard, R. Spitz, J. Claverie, M.F. Llaurro, C. Monnet, Macromolecules 35 (2002) 1513–1523.

[4] (a) Z.B. Guan, Chem. Eur. J. 8 (2002) 3086–3092;
(b) Z.B. Guan, P.M. Cotts, E.F. McCord, S.J. McLain, Science 283 (1999) 2059–2062.

[5] (a) D.H. Camacho, E.V. Salo, Z.B. Guan, Org. Lett. 6 (2004) 865–868;
(b) D.H. Camacho, E.V. Salo, J.W. Ziller, Z.B. Guan, Angew. Chem. Int. Ed. 43 (2004) 1821–1825;
(c) D.H. Camacho, Z.B. Guan, Macromolecules 38 (2005) 2544–2546.

[6] A.S. Ionkin, W.J. Marshall, Organometallics 23 (2004) 3276–3283.

[7] C. Müller, L.J. Ackerman, J.N.H. Reek, P.C.J. Kamer, P.W.N.M. van Leeuwen, J. Am. Chem. Soc. 126 (2004) 14960–14963.

[8] (a) T.R. Younkin, E.F. Connor, J.I. Henderson, S.K. Friedrich, R.H. Grubbs, D.A. Bansleben, Science 287 (2000) 460–462;
(b) C.M. Wang, S. Friedrich, T.R. Younkin, R.T. Li, R.H. Grubbs, D.A. Bansleben, M.W. Day, Organometallics 17 (1998) 3149–3151.

[9] G.M. Sheldrick, SADABS, Program for Empirical Absorption Correction, University of Göttingen, Göttingen, 1996.

[10] A. Altomare, G. Cascarano, C. Giacovazzo, A. Guagliardi, M.C. Burla, G. Polidori, M.J. Camalli, J. Appl. Crystallogr. 27 (1994) 435–436.

[11] G.M. Sheldrick, Shelxl-97-A Computer Program for Refinement of Crystal Structure, University of Göttigen, Göttigen, 1997.

[12] L.J. Farrugia, J. Appl. Crystallogr. 32 (1999) 837–838.

[13] M.N. Burnett, C.K. Johnson, ORTEP-III: Oak Ridge Thermal Ellipsoid Plot Program for Crystal Structure Illustration, Oak Ridge National Laboratory Report ORNL-6895, 1996.

[14] R. Belzen, R.A. Klein, W.J.J. Smeets, A.L. Spek, R. Benedix, C.J. Elsevier, Recl. Trav. Chim. Pays-Bas 115 (1996) 275–285.

[15] E.Y.X. Chen, T.J. Marks, Chem. Rev. 100 (2000) 1391–1434.